

# A Light Scattering based approach for quantification of tissue multifractality: Prospects in pre-cancer detection

## 1. Introduction

Over the last fifty years, there have been tremendous advances in our understanding of the molecular and cellular processes of cancer; however, it still remains to be the deadliest disease of our time. Despite the significant progress made in treatment of a number of neoplastic disorders, early detection of neoplastic changes appears to be our best method to improve patient quality of life and reduce cancer mortality. The conventional methods for early detection and diagnosis of cancer rely on histological and cytological examination of tissue. There is a tremendous need in developing better methodologies for extraction and quantification of the morphological alterations associated with cancer/pre-cancer development. In this regard, the optical spectroscopic and imaging approaches have shown early promise in quantifying both the morphological (using elastic scattering spectroscopy) and biochemical (using inelastic scattering spectroscopy such as fluorescence and Raman) alterations associated with cancer development. Notably, polarized elastic scattering spectroscopy has been explored to quantify the self-similar (fractal) nature of micro-scale fluctuation of local refractive index in tissues <sup>[1]</sup>. These studies have revealed that changes in tissue self-affinity can serve as a potential bio-marker for pre-cancer. Since most of the cancers arise in epithelial tissues, majority of the previous attempts on developing methods (optical or non-optical) for early diagnosis of cancer relied largely on quantifying the alterations in the superficial epithelial layer. However, recently it has been recognized that in addition to the alterations in the superficial epithelial cells, neoplasia is also associated with characteristic changes in the underlying connective tissue layer (stroma). Progression of cancer involves complex interactions between neoplastic cells and the stroma. Also, carcinogenesis results, in part, from defective epithelial - stromal communication. In fact, alterations in stromal biology may precede and stimulate neoplastic progression in pre-invasive disease. Interestingly, the collagen fiber network present in stroma also exhibits fractal architecture in the organization of the fibers and micro-fibrils <sup>[2]</sup>. Quantification of the changes in the fractal characteristics of the stroma may thus provide additional targets to aid in screening and early detection of precancerous changes. With this motivation, we have explored the use of multifractal detrended fluctuation analysis model to extract and quantify the fractal properties of the refractive-index structure (inhomogeneities) in the stromal layer of dysplastic (pre-cancerous) human cervical tissues. The results showed interesting variations in the micro-optical tissue fractal properties in the various states of dysplasia.

## 2. Theoretical background

- **Fractals and multifractals**

A fractal series is one whose variance  $\sigma(x) = \langle |f(x+a) - f(x)|^2 \rangle$ , scales according to  $\sigma(sx) \propto s^H \sigma(x)$ , where H is the Hurst exponent and s denotes the scale, i.e., number of points. The Hurst exponent gives a measure of correlation or anti-correlation behavior between two neighboring points of a fractal series. Values of Hurst exponent =0.5, >0.5 and < 0.5 correspond to uncorrelated random (Brownian) fluctuations, long range correlations or persistent behavior and anti-correlations or anti-persistent behavior respectively. A fractal object is typically characterized by fractional Fractal dimension ( $D_f$ ) which is related to Hurst exponent by a simple equation:  $D_f = D_E - H + 1$  where  $D_E$  is Euclidean dimension. Note that a monofractal series can be generated by computing Fractional Brownian Motion (FBM), i.e., Brownianisation of a white Gaussian noise is a monofractal (this has been used in our control experiments, as described subsequently).

Many of the naturally found objects (and processes as well) exhibit multi-scale self-affinity or multifractality. A multifractal system is a generalization of a monofractal system in which a single exponent (Hurst exponent) is not enough to describe its dynamics; instead, a continuous spectrum of exponents (singularity spectrum) is needed. An exponent  $h(q)$ , function of the order of moment q, is the measure of correlation between consecutive points of a multifractal series. In this case it is termed as Generalized Hurst exponent ( $h(q)$ ). For a stationary series,  $h(q=2)$  is identical with Hurst exponent H. Multifractal series can be generated using a binomial multifractal model that computes a series:  $x_k = a^{n(k-1)}(1-a)^{n_{max}-n(k-1)}$  of  $N = 2^{n_{max}}$  numbers with  $k = 1, \dots, N$ ; where Generalized Hurst exponent is related to the parameter a as exponent  $h(q) = \frac{1}{q} - \frac{\ln\{a^q + (1-a)^q\}}{q \ln 2}$ .

Previously, most of the techniques to detect early cancer relied on quantifying the alterations in superficial epithelial layers of tissues. In present paper, we are going to characterize the changes in fractal properties in connective tissue

layers, i.e., *stromal region*. This is motivated by the recent findings which state that, in addition to the alterations in the superficial epithelial cells, neoplasia is also associated with characteristic changes in the underlying connective tissue layer (stroma). Progression of cancer involves complex interactions between neoplastic cells and the stroma. Also, carcinogenesis, partially, is caused by defective epithelial-stromal communication. In fact, alterations in stromal biology may precede and stimulate neoplastic progression in pre-invasive disease. Interestingly, the collagen fiber networks in stroma also exhibit fractal architecture. Quantification of the changes in the fractal characteristics of the stroma may thus provide additional targets to aid in screening and early detection of precancerous changes. Also, previous efforts have been made to characterize tissue-fractality using light scattering model within *monofractal approximation*. However, as observed by us, the spatial variation of tissue refractive index exhibits multifractality. In order to characterize the tissue-multifractality we thus used a state-of-the-art multifractal analysis method, namely Multifractal Detrended Fluctuation Analysis (MFDFA).

- **Light scattering based model in monofractal approximation**

According to fractal–Born approximation, light scattering signal can be given by the Fourier transform of tissue refractive index (r.i.) spatial correlation function;

$$\mathbf{I}(\boldsymbol{\beta}) \propto \mathbf{k}^4 \int \mathbf{C}(\mathbf{r}) \mathbf{e}^{i\boldsymbol{\beta} \cdot \mathbf{r}} \mathbf{d}^3 \mathbf{r} \quad (1)$$

Where  $\beta$  is the spatial frequency  $= 2k \sin \frac{\theta}{2}$ ,  $\theta$  being the scattering angle, wave vector  $k = \frac{2\pi}{\lambda}$  and  $C(r)$  is the r.i. correlation function.

In order to describe light scattering from self-similar (fractal) biological scatterers, various types of refractive index spatial correlation functions  $C(r)$  have been proposed. Among these, the von Karman self-affine function<sup>[1]</sup>, which is a generalized correlation function for statistically random fractal fields, has been found to be suitable. The von Karman correlation function is given by

$$\mathbf{C}(\mathbf{r}) \propto \left(\frac{r}{l}\right)^H \mathbf{K}_H \left(\frac{r}{l}\right) \quad (2)$$

where  $l$  = fractal upper limit and modified Bessel function of  $2^{\text{nd}}$  kind of the order of  $H$ . The Fourier transformation of the von Karman correlation function thus yields the analytical expression of light scattering signal as

$$\mathbf{F}(\boldsymbol{\beta}) = \mathbf{I}(\boldsymbol{\beta}) \mathbf{k}^{-4} \approx \frac{1}{[1+(\boldsymbol{\beta}l)^2]^\alpha} \quad (3)$$

For  $\beta \gg \frac{1}{l}$ , above relation can be shown to exhibit exact inverse power law behavior  $F(\beta) \propto (l\beta)^{-2\alpha}$  with the scaling exponent  $\alpha$ , Euclidean dimension  $D_E$  and Hurst exponent  $H$  are related as  $\alpha = H + D_E/2$ . Such dependence can be realized by noting that the power spectrum of any fluctuation series is basically the Fourier transform of the autocorrelation function. Thus the Hurst exponent should easily be calculated from the slope of the log-log plot of power spectrum.

In practice, as shown below (Figure 1), the log-log plot of power spectrum of a monofractal (FBM, input Hurst exponent known-a-priori = 0.6) series exhibits linear slope throughout the entire range of frequency (Figure 1a),  $H$ -value obtained from the slope matches the input  $H$ -value of the series. But power spectrum of a multifractal (binomial multifractal, input parameter  $a$  known-a-priori = 0.8) is not at all linear throughout the entire range (Figure 1b); different slopes at different frequency range yield different Hurst exponent values.

This illustrates the inadequacy of Fourier power spectrum based approaches for quantifying multifractality of any non-stationary multi-scaling fluctuation series. Since r.i. fluctuation in tissue shows multifractality (as demonstrated subsequently), the monofractal model (based on Fourier domain analysis) may not be accurate enough to characterize self-similarity for such complex multifractal scattering objects. We have thus used the following strategy for the analysis of light scattering spectrum from multifractal.

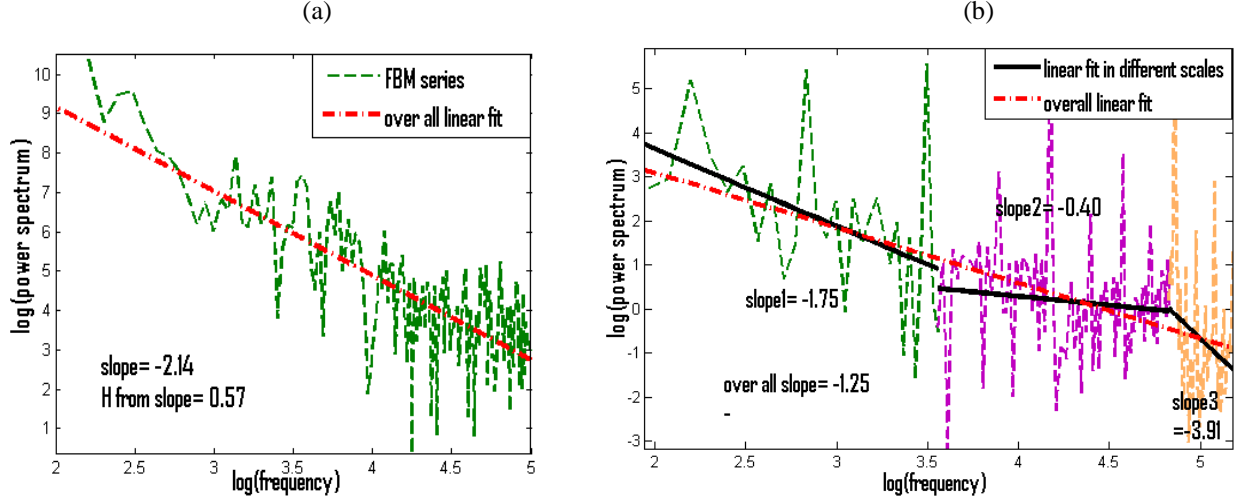


Figure 1. Log-log plot of theoretical power spectrum of (a) monofractal series (FBM) shows linearity throughout the entire range of frequency, Hurst exponent value ( $H = 0.57$ ) calculated from corresponding slope agrees reasonably well with the input H-value ( $=0.6$ ), whereas that of (b) a multifractal series (binomial model) exhibits different slopes in different frequency-range

- **Light scattering based inverse analysis strategy for multifractal**

The multifractal properties in spatial tissue refractive index fluctuations can be analyzed via light scattering signal using the following two approaches.

- 1) Light scattering signal modeled by appropriate multifractal index correlation function;
- 2) An inverse approach to extract representative refractive index fluctuations from light scattering signal.

To model an actual multifractal correlation function is not straightforward. In our present study, we have thus adopted the second approach. The representative fluctuation of refractive index  $\Delta n(r, r')$  can be extracted from the scattering signature using the following approach.

Starting from equation (1), the scattering signal can be expressed as,

$$I(\beta) \propto k^4 \int |\Delta n(r, r') e^{i(\beta \cdot r')} d^3 r|^2 \quad (4)$$

Thus the refractive index fluctuation series can be extracted from the scattering spectra by inverse Fourier transform as

$$\Delta n(r, r') \propto k^{-2} \left| \int \sqrt{I(\beta)} e^{-i(\beta \cdot r')} d^3 \beta \right| \quad (5)$$

Since  $\beta = 2 \cdot \frac{2\pi}{\lambda} \cdot \sin \frac{\theta}{2}$ , the light scattering signal can be recorded either by detecting angular variation of scattering or the wavelength variation of scattering. The resulting representative fluctuation extracted from the light scattering signal (from Eq. 5) can then be subjected to MFDFA, to characterize its multifractality.

- **Multifractal Detrended Fluctuation Analysis (MFDFA)**

MFDFA is a widely used technique to quantify the multifractal parameters namely Generalized Hurst exponent  $h(q)$  and width of singularity spectra  $\Delta\alpha$ . The steps of this method are discussed in details elsewhere [3]. MFDFA, basically, destroys the trend of the given series by subtracting the local polynomial fits and then find the variance (order of moment  $q=2$ ) of the detrended series. From this variance it calculates the  $q$ -th order fluctuation function  $Fq(s)$  and plots it with the length of the data point  $s$ . This variance would exhibit a power law with the length scale if the series is a fractal. This power-law coefficient is termed as Hurst exponent  $h(q)$ . If this  $h(q)$  is the same for all values of order of moment  $q$ , then it is a monofractal series. For a monofractal series,  $h(q)=H$ . On contrary, if  $h(q)$  changes its values for different  $q$ 's, it confirms that the data-series is multifractal. For a stationary multifractal series,  $h(q=2) = H$ . Generalized Hurst exponent is related to classical scaling exponent  $\tau(q)$  via relation  $\tau(q) = qh(q) - 1$ . Another way to characterize multi-fractal series is by singularity spectrum  $f(\alpha)$ , where,  $\alpha$  is singularity strength or Holder exponent and width of singularity spectrum  $\Delta\alpha$  provides a measure of strength of multi-fractality. It is related to  $\tau(q)$  via a Legendre transform, i.e.,  $\alpha = \frac{d\tau(q)}{dq}$  and  $f(\alpha) = q\alpha - \tau(q)$  (Steps for MFDFA are illustrated in case of tissue- index fluctuation in Figure 3).

### 3. Multifractality of tissue

Present point of concern is characterization of tissues. Several studies on this already have revealed that tissues exhibit self-similar behavior or fractality and several efforts were made to establish models to characterize tissue-fractality based on different correlation functions. But all those previous understandings were within monofractal limits whereas it can be proved that tissues basically exhibit multifractality, that is, multi-scale self-similarity and monofractal approximations fail in case of tissue-characterization. The detailed strategy to prove tissue-multifractality can be found in our recently published paper [4]. Tissue-samples used in our experiments are histopathologically characterized biopsy tissue samples of human cervix having different grades of dysplasia (Grade-I, II and III), provided by G.S.V.M. Medical College and Hospital, Kanpur.

- **Analysis of tissue within monofractal approximation: Fourier domain analysis**

The methodology has been described in Section 2 with synthetic fractal images. Likewise, for this analysis, we record Differential Interference Contrast images of tissues and unfold the images in 1-D to obtain the refractive index fluctuation series and plot its Fourier spectrum. Being a statistically self-similar series, it should exhibit a power law ( $F(\beta) \propto (\beta)^{-2\alpha}$ ,  $\beta$  being the spatial frequency here in  $\mu\text{m}^{-1}$ ) at the limit of large. In Figure 2, we show the results of the Fourier analysis on the spatial variation of refractive index from the connective tissue regions of typical dysplastic cervix. The DIC image and the corresponding Fourier power spectra of the generated one dimensional spatial index fluctuations are shown in two consecutive figures. The wide range of sizes and shapes of the inhomogeneities, their high packing densities and other factors all contribute to the complex nature of the

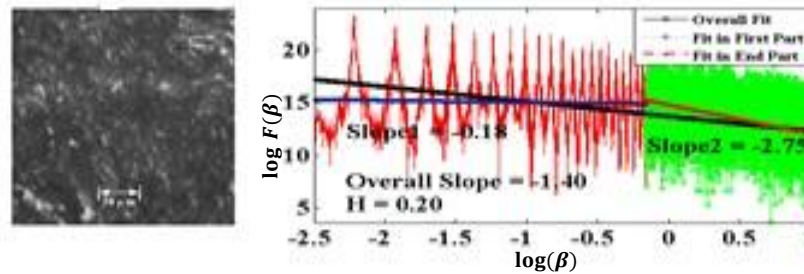


Fig.2 .DIC image of typical grade III dysplastic connective tissues and the corresponding Fourier power spectra of the generated one dimensional spatial index fluctuations are shown. The two different selected frequency ranges (lower and higher) exhibiting different power law scaling are shown by red and green colors respectively. The corresponding fits at lower  $\beta$  range (blue line), at higher  $\beta$  range (red line) and the overall fit (black line) are shown. The values for the power law coefficients (slope  $-2\alpha$ ) and the corresponding estimate for the average Hurst exponents  $H$  (for overall fitting) are noted.

resulting index variations. The power spectra are also associated with large background fluctuations indicating the overall randomness of the underlying index variations. The power spectra exhibit power law scaling beyond a certain spatial frequency range (for  $\beta \geq 0.075 \mu\text{m}^{-1}$ , the spectral density appears linear on a log–log plot), which points towards the fractal nature of tissue-index fluctuation. But, unlike the case for a simple monofractal, the slopes are not the same throughout the entire spatial frequency range. The power law coefficients in different frequency ranges are different, -0.18 and -2.75; either of which are again different from the slope for the entire frequency range (= -1.40). Thus the Fourier domain analysis, i.e., the analysis within monofractal limit is not adequate to parameterize the fractality of tissue properly. It clearly indicates the multifractality of tissue, which can be confirmed from the multifractal analysis on this.

- **Analysis of tissue with multifractal analysis tool: MF DFA**

Failure of monofractal analysis procedure necessitates the application of multifractal analysis procedure. Thus we employ the sophisticated analysis tool MF DFA, which we discussed beforehand, on the one dimensional index fluctuation series. In Figure 3, the steps of MF DFA on unfolded refractive index fluctuation series extracted from the DIC image of a typical Grade-I dysplastic tissue are shown.

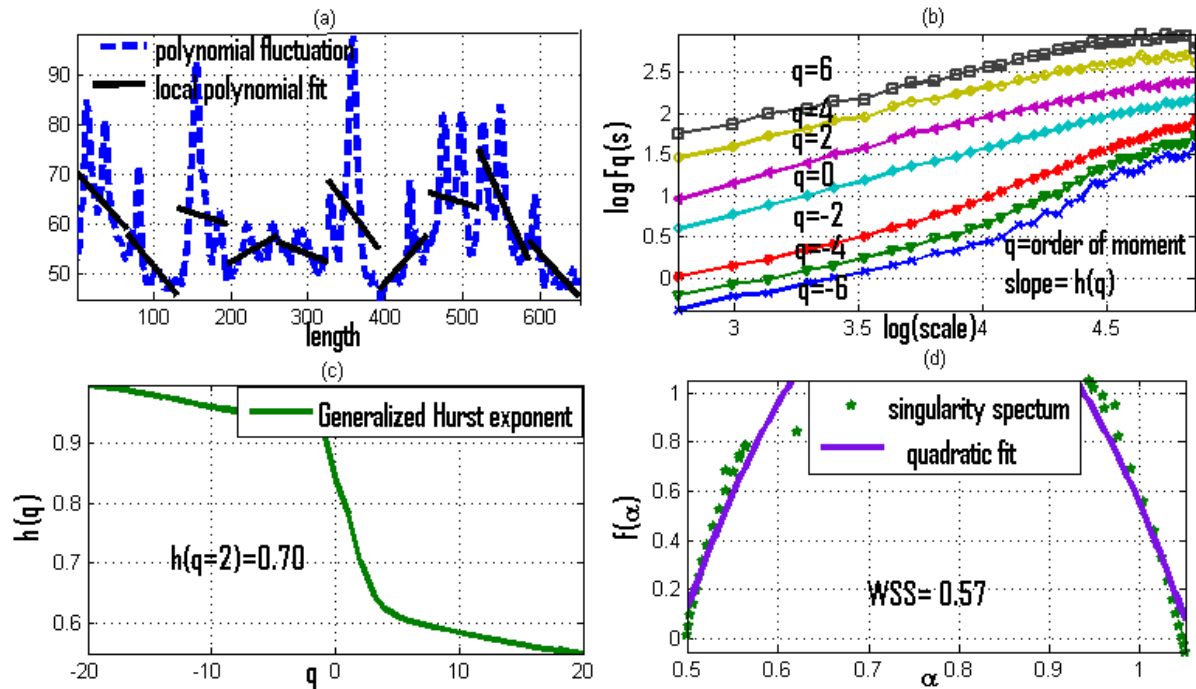


Figure 3: With the 1-D fluctuation series obtained from a typical DIC image of a grade-I dysplastic tissue. The detrending procedure is shown in (a). Blue dotted line is the original data and the black lines are the fitted data. Detrended series is obtained by subtracting the fitted data from the original one. The  $q$ -th order fluctuation function  $F_q$  is plotted against length of data points in log-log scale (b), exhibiting different slopes for different orders of moment. Plots for Generalized Hurst exponent and Width of Singularity are shown in (c) and (d).

It is shown clearly that the slope, i.e., the Hurst exponent  $h(q)$  values are changing significantly with order of moment  $q$ . It is a clear confirmation of multifractality in index fluctuation. Also the sigmoid nature of the Generalized Hurst exponent curve and the width of multifractality are in excellent agreement with this observation. Thus it is proved that tissues are multifractals and no monofractal-assumption based analysis procedure can be able to characterize it. It obviates the need of the alternative analysis strategy, i.e., the inverse analysis strategy that we already have discussed in Section 2. Also, it is seen that variation in slope is larger for negative  $q$  values than that for

positive q-values. Again, negative q amplifies small-scale fluctuations more. Thus the variation in result for different grades of dysplasia is expected mainly from the small-scale fluctuation regime.

#### 4. Experimental strategy: Light scattering based approach for quantification of tissue-multifractality

Our ultimate goal is to look for a non-invasive methodology for quantitative detection of early cancer. Thus preparing tissue slides and taking microscopic images cannot be preferred. Consequently we cannot move with DIC imaging. In this case, light scattering spectroscopic measurement can serve our purpose. In order to establish the light scattering based experimental strategy, we first validate our strategy through control experiments with synthetic mono-fractals and multifractals and then come to experiment with actual tissue. As described earlier, the scattering intensity can be measured from both wavelength and angular variation. Here, in the control experiment, the scattering intensity is recorded as the angular variation of scattering and in case of tissues, it is recorded as the wavelength variation of scattering.

- **Validation through control experiment**

Schematic diagram in Figure 4 presents the set-up for measurement of angular variation of scattering. The Twisted Nematic Spatial Light Modulator (TN-SLM, LC – R 2500; Holoeye Photonics, Germany, *number of pixel*  $800 \times 600$ , *pixel size*  $32 \mu\text{m}$ ) is serving as the scattering object here. Processed fractal phase map (2-D images of monofractal FBM and Binary multifractal series, having different Hurst exponent values which are user controlled and known-a-priori) are relayed through the SLM, working in forward geometry. The angular distribution of the scattered light is obtained from the detected light intensity at individual pixels of EMCCD (Andor iXon3-885, number of pixels =  $1004 \times 1002$ , pixel area =  $8 \times 8 \mu\text{m}^2$ ) along the horizontal direction (illustrated separately).

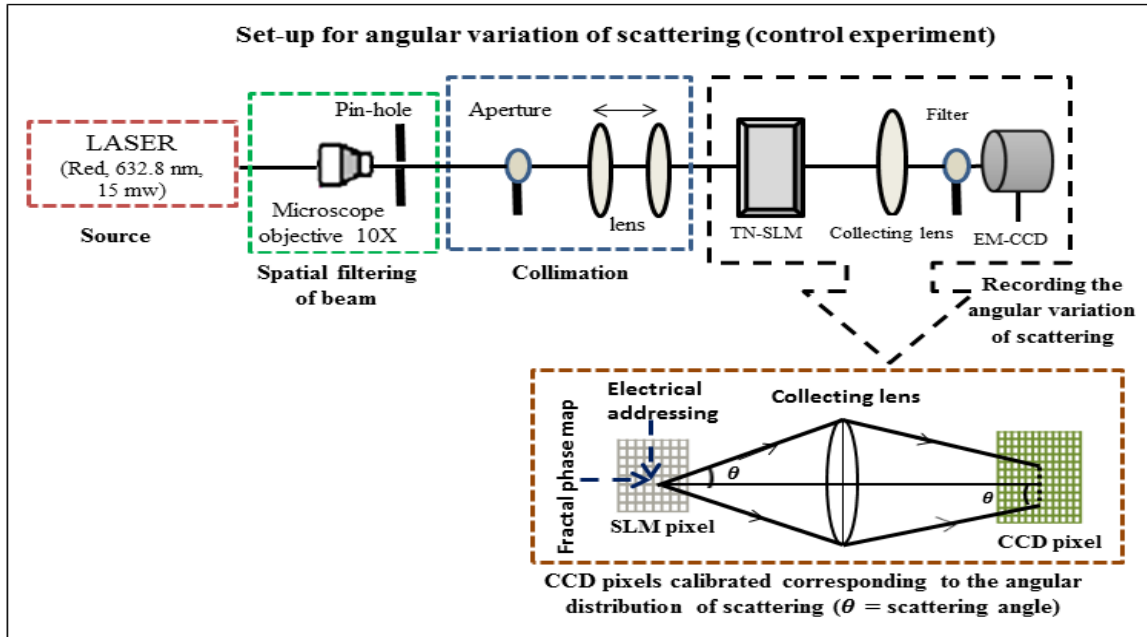


Figure 4: A schematic of the experimental set-up for the measurement of angular variation of light scattering

- **Experiment with actual tissue:**

Similar procedure as above is applied on actual with actual tissues (slides prepared with unstrained tissue sections of thickness  $\sim 5 \mu\text{m}$ , lateral dimension  $\sim 4 \text{ mm} \times 6 \text{ mm}$ ). The scattering intensity is recorded by the Fiber-optic spectrometer as the function of wavelength variation (400-700nm), as shown in the schematic Figure 5. We are specifically interested in backward scattering region since the small-scale fluctuations dominate in the backward scattering and also due to the ease of practical setup with patient.

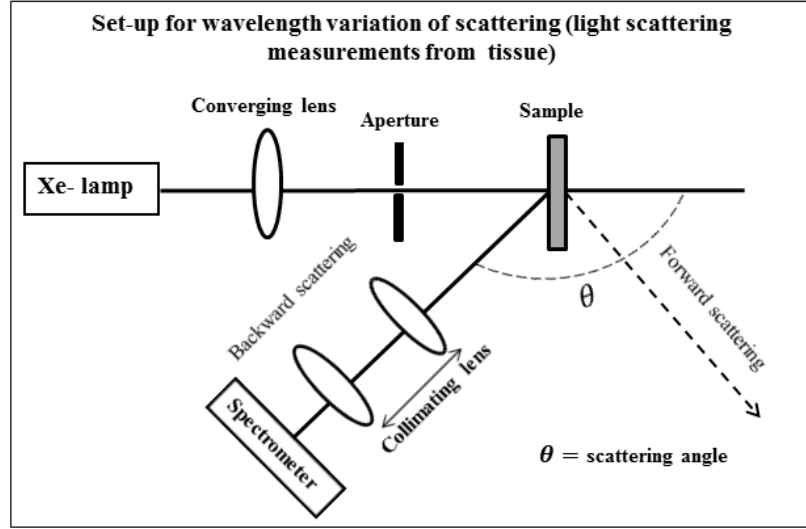


Figure 5: A schematic of the experimental set-up for the measurement of wavelength variation of light scattering

## 5. Results and Discussions

In control experiments with multifractal series, the Generalized Hurst exponent of the series extracted by inverse analysis from theoretical power spectrum and experimental light scattering signal for a multifractal series of input parameter  $a = 0.8$  are shown in the figure 6 which exhibits the agreement in the value of Hurst exponent estimated from both (only one result is shown here though we have dealt with different images of series having  $0.5 < a < 1$ ). Slight discrepancy observed may be due to limited size of the fractal series used since MFDFA gives accurate results for statistically large series only. However, in our case, the series was restricted by the pixel dimensions of the SLM ( $800 \times 600$ ). Never-the-less, good agreement is observed between the multifractality quantified via the inverse analysis of light scattering signal and the corresponding theoretical analysis of the input multifractal. This therefore validates our light scattering inverse analysis strategy for quantification of multifractality.

We also have done the same analysis with synthetic monofractal FBM images with input Hurst exponent known-a-priori ( $0.1 < H < 1.0$ ). Those have been analyzed with the Fourier domain analysis method, using von-Karman correlation function based monofractal assumption. The results are shown in Table 1 (results shown only for lower H-values, for  $H > 0.6$  the FBM series generated by inbuilt MATLAB program is not a proper monofractal, some multifractality can also be found, so results could come inappropriate).

Table 1: Results of the control experiment with monofractal (FBM) showing the similarity in values of Hurst exponent calculated from the log-log plot analysis of theoretical power spectrum and experimental light scattering data

Input Hurst exponent	Slope of theoretical power spectrum log-log plot = $-(2H+1)$	H from theoretical power spectrum	Slope of experimental light scattering data, log-log plot = $-(2H+2)$	H from experimental light scattering data
0.1	-1.12	0.06	-2.18	0.09
0.2	-1.25	0.12	-2.28	0.14
0.3	-1.40	0.20	-2.48	0.24
0.4	-2.02	0.51	-2.87	0.44
0.5	-1.96	0.48	-2.95	0.48
0.6	-2.13	0.56	-3.14	0.57

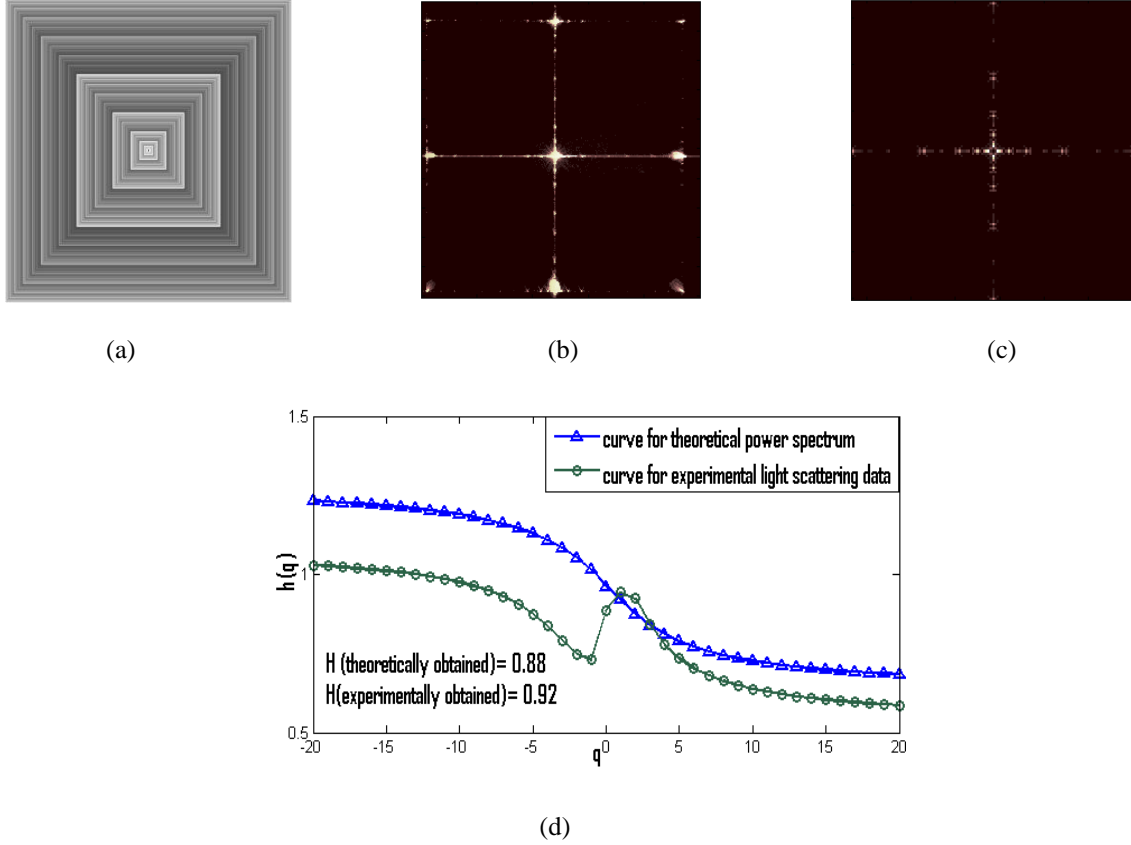


Figure 6: 2-D image of binomial multifractal is processed (a). Its theoretical power spectrum (b) is analyzed and experimental scattering signal (c) is recorded. The fluctuation series is obtained by inverse analysis. MFDFA on those series give the Generalized Hurst exponent plot,  $h(q=2) = H$  (d).

Thus, for both monofractal and multifractal, theoretical and experimental values of fractal-parameter are in proper agreement which, in turn, validates our experimental strategy.

Now we apply this strategy on actual tissues. The results obtained from the Inverse analysis of light scattering spectra from tissues show a clear deviation in Hurst exponent and increase in width of multifractality for higher grades of pre-cancer. Table-2 gives the comparative study on 29 tissue-samples having different grades of pre-cancer.

Table 2. Summary of the MFDFA analysis on the spatial refractive index fluctuations in DIC images connective tissue regions of the human cervix specimens with different grades of precancers (dysplasia).

Tissue region	Generalized Hurst exponent $h(q=2)$			Width of singularity spectra $\Delta\alpha$		
	Grade I	Grade II	Grade III	Grade I	Grade II	Grade III
<b>Connective tissue</b>	$0.54 \pm 0.03$	$0.50 \pm 0.04$	$0.36 \pm 0.08$	$0.60 \pm 0.10$	$0.68 \pm 0.13$	$0.88 \pm 0.07$

Clear trend is apparent for higher grades of pre-cancer. Decrease in Hurst exponent for higher grades of precancer indicates the anti-persistent behavior of index fluctuations within the tissue which may originate due to the fact the fibrous network present in connective tissue region gets disturbed in diseased condition, fibers tend to get shortened and correlation breaks. Increase in width of singularity spectrum also indicates the increasing roughness due to increase in disease in sub-cellular level.



The initial application of our experimental strategy underscores its promises to be employed as a non-invasive tool for detection as well as quantification of pre-cancer. We are able to prove our technique accurate through control experiments and to explain the results we observed from application of the strategy on tissues reasonably. The successful application of the methodology, thus, states its relevance and significance in terms of quantitative measurement of pre-cancer.

References:

- [1] M. Hunter, V. Backman, G. Popescu, M. Kalashnikov, C. W. Boone, A. Wax, V. Gopal, K. Badizadegan, G. D. Stoner, and M. S. Feld, "Tissue self-affinity and polarized light scattering in the Born approximation: A new model for precancer detection," *Phys. Rev. Lett.*, vol. 97, no. 13, p. 138102, Sep 2006.
- [2] D. Arifler, I. Pavlova, A. Gillenwater, and R. Richards-Kortum, "Light scattering from collagen fiber networks: Micro-optical properties of normal and neoplastic stroma," *Biophysical Journal*, vol. 92, no. 9, pp. 3260 – 3274, 2007.
- [3] J. W. Kantelhardt, S. A. Zschiegner, E. Koscielny-Bunde, S. Havlin, A. Bunde, S. Havlin, H. E. Stanley, "Multifractal detrended fluctuation analysis of nonstationary time series", *Physica A*, **316**, 87 (2002).
- [4] N. Das, S. Chatterjee, J. Soni, J. Jagtap, A. Pradhan, T. K. Sengupta, P. K. Panigrahi, I. Alex Vitkin, and N. Ghosh "Probing multifractality in tissue refractive index: prospects for precancer detection"; *Opt. Lett.*, Vol. 38, Issue 2, pp. 211-213 (January 2013).